J. Quant. Spectrosc. Radiat. Transfer, Vol. 18, pp. 573–580. Pergamon Press 1977. Printed in Great Britain

RELAXATION OF THE Ne($2p_1$) LEVEL AND POPULATIONS OF Ne($1s_2$) AND Ne($1s_4$) IN AN AFTERGLOW

ANDRÉ MONTEIL, JACQUES CHEVALEYRE, ANNIE BOUVIER and JOSEPH JANIN
Laboratoire de Spectroscopie et de Luminescence, E.R.A. C.N.R.S. No. 302, Université Claude Bernard-Lyon I, 43, Bd du 11 Novembre 1918, 69621-Villeurbanne, France

(*Received* 1 *February* 1977)

Abstract—Radiation trapping of the transition $2p_1 - 1s_2$ of neon has been demonstrated during laser-induced fluorescence in a pulsed microwave discharge through neon. The population of Ne($1s_2$) atoms is deduced. Selective excitation is useful for the determination of lifetimes and cross sections of collisions with neutral atoms. The results may be utilized in processes for the creation of metastable atoms.

1. INTRODUCTION

MEASUREMENTS of relaxation rates for neon resonance levels showed that strong radiation trapping occurred. DECOMPS[1] studied this phenomenon for Ne($3s_2$) and BOUVIER[2] for the Ne($1s_2$) and ($1s_4$) levels. For the $1s_4$ level, radiation trapping rose to 99%.

This effect is important for lines coupled with the ground state. Because of the relative importance of metastable atom populations (about 10^{11} atoms/cm^3 in discharges), we thought it was possible to observe this effect for lines coupled with metastable levels. In fact, experimental relaxation-rate measurements in d.c. discharges for transitions where the lower level is metastable, are longer than is expected theoretically. According to DUCLOY[3] and CARRINGTON,[4] this is due to "radiation trapping".

In this work we investigate radiation trapping for the $2p_1 - 1s_2$ neon transition by determining the variation of the Ne($2p_1$) relaxation rate as a function of metastable atom population, using a pulsed discharge afterglow and knowing that the metastable Ne($1s$) population is time-dependent and its relaxation rate is much higher than that of Ne($2p_1$). An energy-level diagram for neon is given in Fig. 1.

2. EXPERIMENTAL SET-UP

Neon contained in a spherical cell (13 cm diameter) is excited by a pulsed microwave discharge (during 1 or 2 μs for $\lambda = 3.1$ cm, produced by a 144 kW generator at frequencies of 400 or 800 Hz). In the afterglow, a large metastable Ne($1s$) population exists which reaches a maximum 100 μs after the discharge, while other excited neon levels are unpopulated.

The laser pulse [$\lambda = 5401$ Å, Ne($1s_4 - 2p_1$)] is produced during the afterglow by an AVCO Everett 950 A neon laser (flash duration = 3 ns, peak power = 10 kW), working at a maximum repetition rate of 100 Hz. The Ne($2p_1$) level is selectively populated and we have studied its relaxation rate, avoiding radiative and collisional cascades.

A frequency divider associated with a delay line permits setting the laser pulse at various times during the afterglow. The fluorescence light is received by a Jobin-Yvon H 20 V monochromator and a 56 DUVP R.T.C. photomultiplier. The signal is sampled and integrated with a boxcar integrator P.A.R. 163 mounted with an S-3A sampling head (bandwidth = 1 GHz). Measurements can be made during 100 ns through a 5 ns gate.

3. EFFECT OF TRAPPING ON EXCITED-LEVEL RELAXATION

(a) *Theory*

The relaxation rate τ is given by

$$1/\tau = \Gamma = \gamma + Cp - \gamma \sum_i \Lambda_i x_i. \tag{1}$$

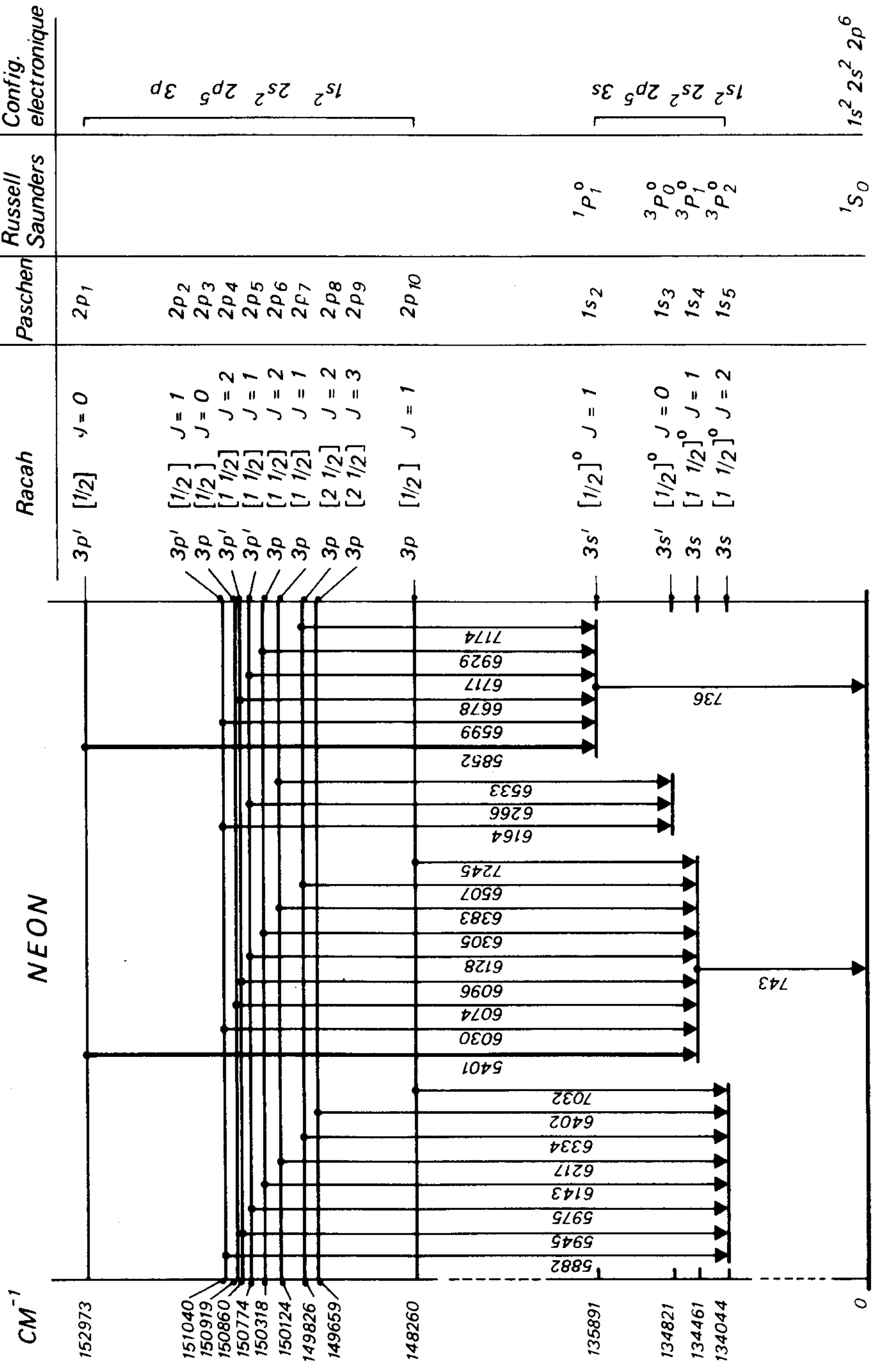

Fig. 1. Energy level diagram for neon.

Here, the first term γ represents the deexcitation by spontaneous emission and $1/\gamma$ is the radiative lifetime of the upper level; the second term Cp represents deexcitation by atomic collisions, which is proportional to the neutral atom pressure p for $p < 10$ torr; the third term $\gamma\sum_i \Lambda_i x_i$ represents the trapping contribution to the population of the upper level (Λ_i is the branching ratio for the ith line from the $2p_1$ level and x_i is the radiation-trapping coefficient). We deduced the Λ_i from the transition probabilities calculated by FENEUILLE[5] for the two lines coming from the $2p_1$ level [for $2p_1 - 1s_4$, the transition probability[5] is $0.75 \times 10^6\,\mathrm{s}^{-1}$ and $\Lambda_i = 0.01$; for $2p_1 - 1s_2$, the transition probability[5] is $74.45 \times 10^6\,\mathrm{s}^{-1}$ and $\Lambda_i = 0.99$]. Neglecting Λ_i for the $2p_1 - 1s_4$ transition, eqn (1) becomes

$$\Gamma = \gamma + Cp - \gamma x_{2p_1-1s_2}. \tag{2}$$

The radiation trapping coefficient x was calculated by HOLSTEIN,[6] DYAKONOV and PEREL,[7] and by OMONT.[8] It is given by

$$x = 1 - \frac{1}{\sqrt{\pi}} \int_{-\infty}^{+\infty} \exp(-t^2) \exp[-k_0 l \exp(-t^2)]\,\mathrm{d}t, \tag{3}$$

where l characterizes the optical path, k_0 is the absorption coefficient for the center of the Doppler line profile and is given by

$$k_0 = \frac{g_u}{g_l} \frac{\lambda^3 N \gamma}{8\pi} \left(\frac{m}{2\pi kT}\right)^{1/2}, \tag{4}$$

λ is the wavelength, N = the lower level population, m = the atomic mass, T = the gas temperature, and g_u and g_l are the statistical weights of the upper and lower levels, respectively. For $k_0 l < 0.1$ (thin-gas limit), x is approximately

$$x = k_0 l/\sqrt{2}, \tag{5}$$

i.e. x is proportional to N and therefore to the partial pressure p^* of Ne($1s_2$) since $N = p^*/kT$. Letting

$$K = \frac{l}{2} \frac{g_u}{g_l} \lambda^3 \gamma^2 \frac{m^{1/2}}{(4\pi kT)^{3/2}}, \tag{6}$$

we obtain $\gamma x = Kp^*$. Hence, eqn (2) becomes

$$\Gamma = \gamma + Cp - Kp^*. \tag{7}$$

(b) *Experimental studies*

We know that the partial pressure of $1s_2$ atoms is time-dependent after the discharge. In order to study Γ as a function of p^*, we have plotted Γ as a function of t_R in Fig. 2, where t_R is the time interval between the microwave discharge and laser excitation.

These experiments were done for several total pressures p.

4. RESULTS ON TRAPPING

The experimental curves (Fig. 2) show, for large values of t_R ($t_R > 200\,\mu$s), that the metastable-atom population decreases continuously with time. Each curve has the asymptote $\Gamma_{\lim} = \gamma + Cp$, where $\Gamma_{\lim}$ is used to determine the lifetime and cross section of the $2p_1$ level.[9] For small values of t_R ($t_R < 200\,\mu$s), the experimental points stay under the asymptote because of reabsorption by metastable atoms $1s_2$ [corresponding to the term $-Kp^*$ in eqn (7)]. Thus, we show reabsorption by Ne($1s_2$) atoms of the line $\lambda = 5852$ Å ($2p_1 - 1s_2$).

The discrepancies between the curves $\Gamma = f(t_R)$ and the asymptotes give the reabsorption x_i, from which we deduce the value of $k_0 l$ from tables[10] established for eqn (3).

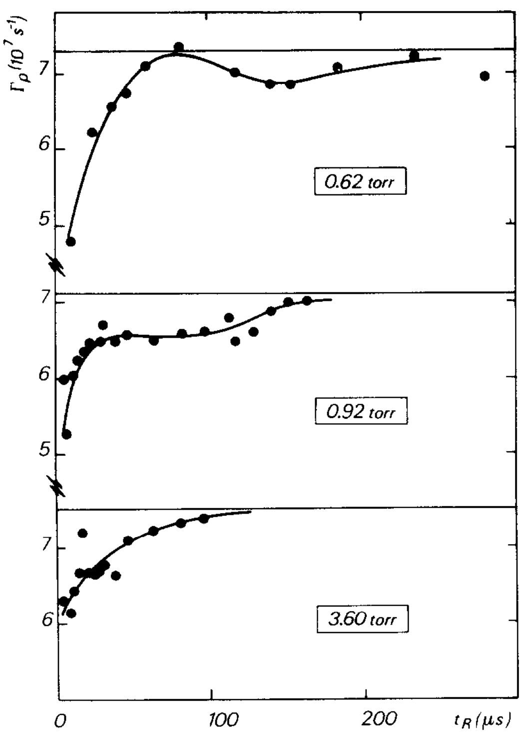

Fig. 2.

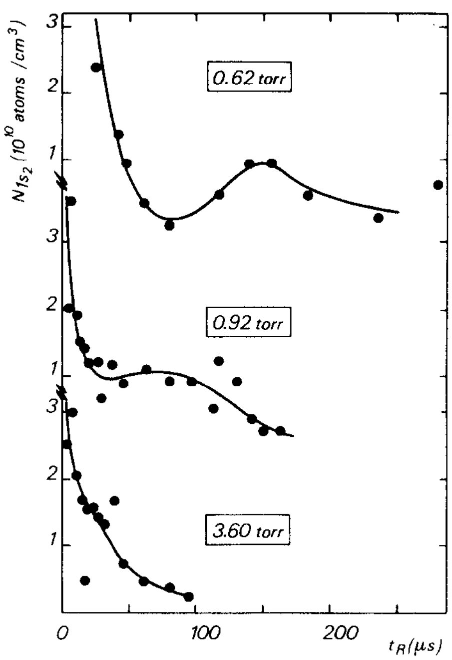

Fig. 3.

Fig. 2. The relaxation rate of the $2p_1$ population as a function of the time after discharge for several neon pressures.

Fig. 3. The $1s_2$ population as a function of the time t_R between the discharge and the laser pulse.

To obtain an estimated value of the population, we consider a homogeneous discharge over a 0.1 m length at $T = 1000$ K, using Doppler profiles from Lardy.[11] From eqn (4) with $\gamma = 7.1 \times 10^7 \text{ s}^{-1}$, $g_u = g_{2p_1} = 1$, $g_l = g_{1s_2} = 3$ and $\lambda = 5852$ Å, we find the Ne($1s_2$) population. Its variations with t_R are plotted for values of the pressure p in Fig. 3. For $p = 0.92$ torr, the Ne($1s_2$) concentration is about 3×10^{10} cm^{-3} immediately after the discharge.

5. LIFETIME AND CROSS SECTION

Figure 4 is obtained by plotting $\Gamma_{\text{lim}} = \gamma + Cp$ as a function of the pressure and gives the lifetime $1/\gamma$ by extrapolation to zero pressure and the cross section σ for deexcitation by neutral atoms. Knowing that $Cp = n\sigma\langle v\rangle$, $\langle v\rangle = \sqrt{8kT/\pi m}$ and $n = p/kT$, the slightly positive slope C of Fig. 4 gives

$$\sigma = C\sqrt{\pi mkT/8}.$$

We find $1/\gamma = (14.1 \pm 0.4)$ ns, $\sigma = (0.2 \pm 0.3)10^{-15}$ cm^2. Among the published values for γ,[3,12–18] ours is closest to the theoretical calculations of Feneuille *et al.*[5] and Gruzdev and Loginov.[19] The mean value 0.2×10^{-15} cm^2 obtained for the neon deexcitation cross section is smaller than $(3.3 \pm 4)10^{-15}$ cm^2 [see Ref. (17)]. Our improved accuracy may be due to the use of a larger Ne-pressure range. We explain the low value obtained for σ by the fact that the $2p_1$ level is far removed from the other $2p$ levels; the nearest level ($2p_2$) is at 1933 cm^{-1}, which represents 3 kT for $T = 1000$ K;[11] therefore, the $2p_1$ level is not easily deexcited.

6. EVOLUTION OF THE Ne($1s_4$) POPULATION

The Ne($1s_4$) population is connected to the maximum fluorescence intensity I_F of the line ($2p_1 - 1s_2$) and to the reabsorption rate x by the following expression:

$$N_{1s_4} = \mathcal{K} I_F/(1 - x),$$

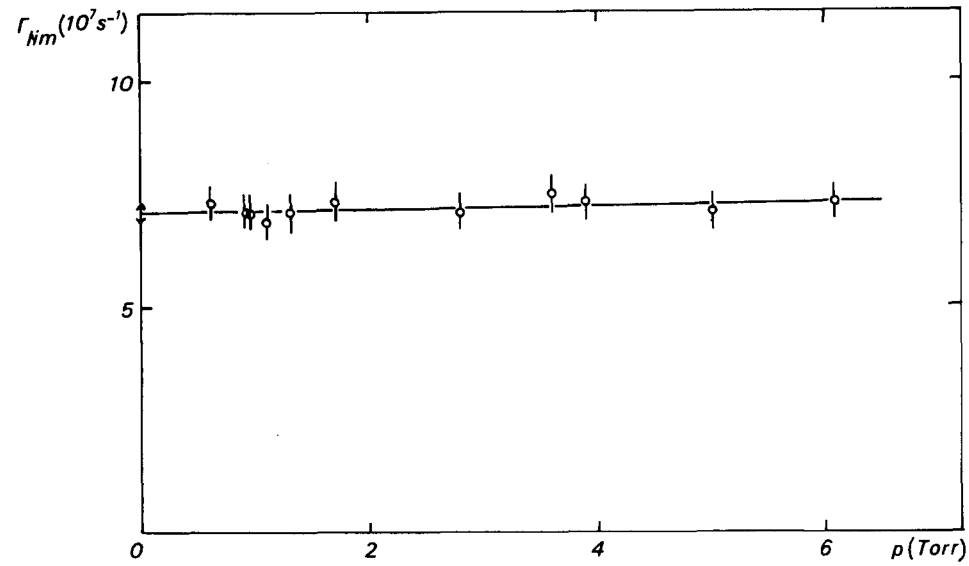

Fig. 4. The relaxation rate of the $2p_1$ population as a function of the neon pressure (the trapping effect has been removed).

where $\mathscr{K}$ is a proportionality coefficient. In Fig. 5, we plot the N_{1s_4} population variation against t_R for different neon pressures p. The curve shapes are similar to those obtained by the absorption method.[2] Our measurements should be more accurate than BOUVIER's,[2] which were obtained during the first few microseconds after the discharge. Absorption measurements are difficult to perform when the population of the lower level is high; emission measurements are better when the emission intensity is stronger.

We notice on the curves connected with the lower pressures a decrease of the population during the first tens of microseconds after the discharge, which suggests the existence of a

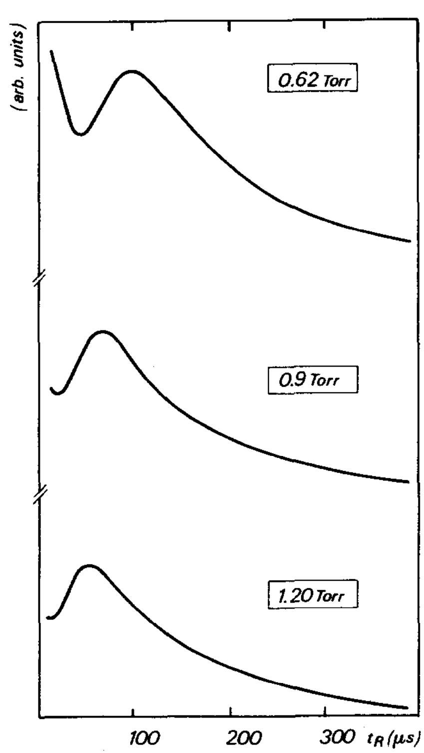

Fig. 5. The $1s_4$ population as a function of the time t_R.

maximum a few microseconds before beginning of the the measurements (because the metastable population is extremely weak before the discharge).

There is a strong analogy between the population variation curves for $1s_2$ and $1s_4$ neon atoms. In particular, both show for lower pressures a maximum around 100 μs after the discharge; we also notice for both levels an initial decrease of population. The mean difference in the temporal behavior of the two populations is the result of the faster relaxation rate of the $1s_2$ level. This result was already known;[11] it is explained by the relatively large difference of energy between $1s_2$ and the other $1s$ states, which implies a weaker coupling with the metastable levels $1s_5$ and $1s_3$.

7. MECHANISMS POPULATING THE $1s_2$ AND $1s_4$ LEVELS

The two population maxima (discharge and afterglow) for Ne($1s$) may be compared with the two intensity maxima for the emission of lines from the $2p$ levels (Fig. 6). We see that the two population maxima are similar, while the second intensity maximum is much weaker than the first. If the Ne($2p$) and Ne($1s$) formation mechanisms are identical, their efficiencies must be different.

The two maxima found for the $1s$ population indicate the presence of two processes. We attribute the maximum occurring for Ne($1s_4$) immediately after the discharge to radiative cascades towards $1s$ levels. The population n of a $1s$ level is related to the intensities $I_i(t)$ of the transitions to this level by

$$\frac{dn}{dt} = \sum_i \alpha_i I_i(t) - \beta n, \tag{8}$$

where the constants α_i relate intensities I_i to the populations of upper levels and β is the decay constant of the $1s$ level through diffusion and collision effects; β is of the order of $10^4\ \mathrm{s}^{-1}$.[2] $I_i(t)$ is large during the discharge and the second member of eqn (8) is positive, thus causing an initial increase. At the end of the discharge, the emission decreases substantially, $\sum_i \alpha_i I_i(t)$ becomes smaller than βn and n decreases. Thus, the population goes through a maximum at

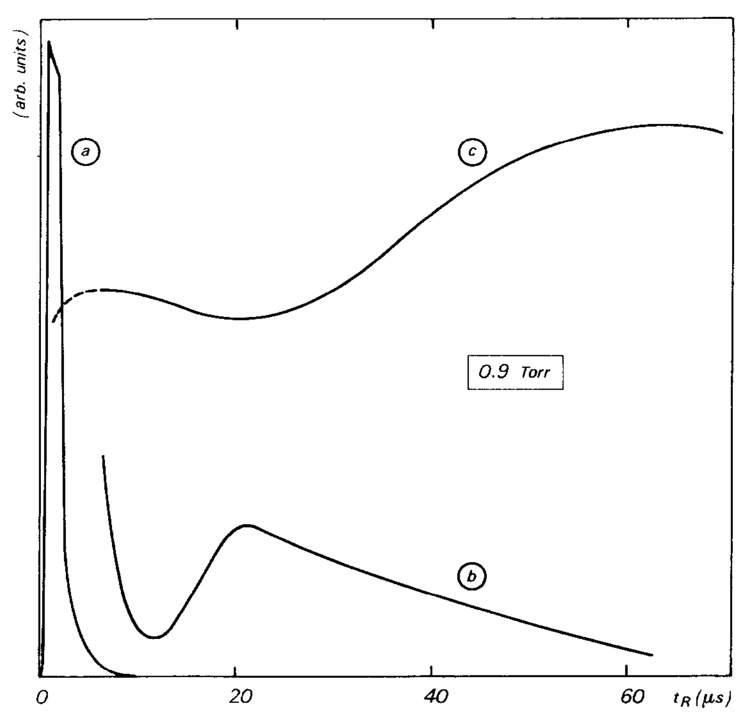

Fig. 6. (a) Emission intensity for the line 6096 Å ($2p_4 - 1s_4$); (b) the same curve amplified; (c) the ($1s_4$) level population.

about the time where the emission is a minimum. This time behavior is shown in Fig. 6 for the line $\lambda = 6096$ Å ($2p_1 - 1s_4$).

The second maximum in the Ne($1s$) population may be attributed to recombination processes leading to excited levels. The main processes are dissociative recombination,

$$Ne_2^+ + e^- \longrightarrow Ne^* + Ne \longrightarrow Ne + Ne + h\nu, \tag{9}$$

and collisional radiative recombination,

$$Ne^+ + e^- \longrightarrow Ne^* \longrightarrow Ne + h\nu. \tag{10}$$

According to SAUTER *et al.*,[20] process (9) occurs more frequently during the afterglow because a greater proportion of molecular ions is present. Sauter *et al.* also note that process (9) leads to lower-level excitations, while process (10) is more efficient in producing higher-level excitations. Process (10) would then explain the intensity maximum observed soon after the discharge while process (9) accounts for the $1s$ population maximum in the afterglow.

Figures 3 and 5 show that the maximum of the Ne($1s_2$) and Ne($1s_4$) populations occur earlier when the pressure p is increased. At high pressures, the maximum is lost in the population decay observed at the end of the discharge. Figure 7 summarizes the results obtained with the $1s_4$ level. The displacement of the maximum with increasing pressure reflects an increase of the recombination coefficient due to decreasing electronic temperature, and also an increase of the population of Ne_2^+ ions through the conversion mechanism

$$Ne^+ + 2Ne \longrightarrow Ne_2^+ + Ne.$$

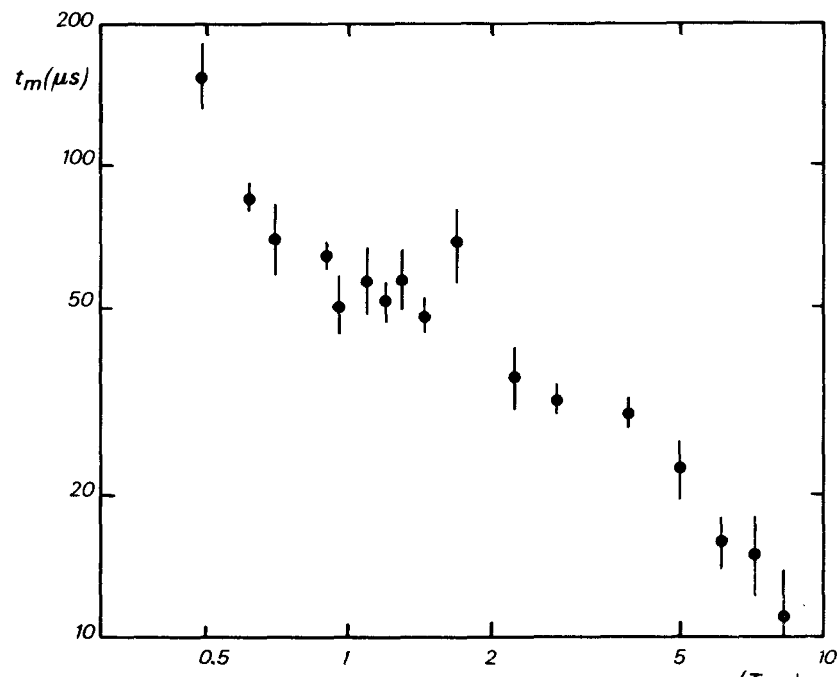

Fig. 7. Variation of the time t_m of the $1s_4$ population maximum as a function of the neon pressure.

8. CONCLUSION

Our results demonstrate the existence of trapping effects for transitions coupled to metastable levels. Trapping is expressed by the Kp^* term [eqn (7)], which represents the distance between the curve and asymptote. This is integrated along the path of the discharge, which is inhomogeneous and optically thin.

Our method for determining lifetimes and cross sections in pulsed discharges is of interest, because the trapping effect can be checked directly. This would be impossible using d.c. discharges since Γ cannot be extrapolated to zero metastable populations.

REFERENCES

1. B. DECOMPS, Thèse de Doctorat ès Sciences, Paris (1969).
2. A. BOUVIER, Thèse de Doctorat ès Sciences, Lyon (1971).
3. M. DUCLOY, *Ann. Phys.* **8**, 403 (1973–74).
4. C. G. CARRINGTON, *J. Phys.* **B5**, 1572 (1972).
5. S. FENEUILLE, M. KLAPISH, E. KOENIG and S. LIBERMAN, *Physics* **48**, 571 (1970).
6. T. HOLSTEIN, *Phys. Rev.* **72**, 1212 (1947).
7. M. I. DYAKONOV and V. I. PEREL, *Soviet Physics JETP* **20**, 997 (1965).
8. A. OMONT, Thèse de Doctorat ès Sciences, Paris (1967).
9. A. MONTEIL, A. BOUVIER and J. CHEVALEYRE, *C.R. Acad. Sci. Paris* **282B**, 3, 91 (1976).
10. M. C. BAJARD, Thèse de Doctorat de Spécialité, Lyon (1972).
11. J. P. LARDY, Thèse de Doctorat de Spécialité, Lyon (1976).
12. G. E. ASSOUSA, L. BROWN and W. K. FORD, *JOSA* **60**, 1311 (1970).
13. A. DENIS, J. DESESQUELLES and M. DUFAY, *C.R. Acad. Sci. Paris* **266B**, 1016 (1968).
14. J. Z. KLOSE, *Phys. Rev.* **141**, 181 (1966).
15. J. BAKOS and J. SZIGETI, *Opt. Spectrosc.* **23**, 255 (1967).
16. A. L. OSHEROVICH and Y. F. VEROLAINEN, *Opt. Spectrosc.* **22**, 181 (1967).
17. W. R. BENNETT and P. J. KINDLMANN, *Phys. Rev.* **149**, 38 (1966).
18. A. POCHAT, M. DORITCH and J. PERESSE, *J. Chem. Phys.* **70**, 976 (1973).
19. P. F. GRUZDEV and A. Y. LOGINOV, *Opt. Spectrosc.* **35**, 1 (1973).
20. G. F. SAUTER, R. A. GERBER and H. L. OSKAM, *Physica* **32**, 1921 (1966).